

Control of power generated by a floating offshore wind turbine perturbed by sea waves

L. Pustina ^a, C. Lugni ^{b,c,d}, G. Bernardini ^{a,b}, J. Serafini ^a, M. Gennaretti ^{a,b,e,*}

^a Department of Engineering, Roma Tre University, Via Della Vasca Navale 79, 00146, Rome, Italy

^b INM-CNR, The Italian Ship Model Basin, Via di Vallerano 139, 00128, Rome, Italy

^c NTNU-AMOS, Center for Autonomous Marine Operation Systems, Trondheim, Norway

^d Institute of Marine Hydrodynamics, Harbin Engineering University, Harbin, China

^e IAS-CNR, Istituto per lo studio degli impatti Antropici e Sostenibilità in ambiente marino, Via Della Vasca Navale 79, 00146 Rome, Italy



ARTICLE INFO

Keywords:

Wind turbine
Floating offshore platform
Sea-wave/platform interaction
Aero-hydro-mechanics modeling
Energy harvesting
Control of stability and response

ABSTRACT

Offshore wind energy is expected to provide a significant contribution to the achievement of the European Renewable Energy targets. One of the main technological issues affecting floating offshore wind turbines concerns generated power fluctuations and structural fatigue caused by sea-wave/platform interactions. This paper presents a fully-coupled aero/hydro/servo-mechanic model for response and control of floating offshore wind turbines in waves, suitable for preliminary design. The wind-turbine is described by a multibody model consisting of rigid bodies (blades and tower) connected by hinges equipped with springs and dampers (for realistic low-frequency simulation). The aerodynamic loads are evaluated through a sectional aerodynamic approach coupled with a wake inflow model. A spar buoy floating structure supports the wind turbine. The hydrodynamic forces are evaluated through a linear frequency-domain potential solver, with the free surface deformation effects included through a reduced-order, state-space model. An optimal controller is identified and applied for rejection of annoying fluctuations of extracted power and structural loads. The developed comprehensive model has been successfully applied to a floating version of the NREL 5 MW wind turbine for stability analysis, as well as for the analysis of uncontrolled and controlled responses to regular and irregular short-crested sea waves. The proposed controller, based on the combined use of blade pitch and generator torque as control variables and the application of an observer for non-measurable aerodynamic and hydrodynamic states estimation, has been demonstrated to be effective in a wide frequency range for alleviation of both generated power fluctuations and vibratory loads.

1. Introduction

The 2050 low carbon economy target requires a constant growth of the energy harvesting by renewable sources. The climate and energy package, setting the binding legislation to ensure that the European Union (EU) achieves its climate and energy goals, indicates the key target of 32% of energy from renewable resources within 2030 [1]. EU identifies the wind and the photovoltaic technologies as the most promising ones. Concerning the wind, the installed power in EU at the beginning of 2018 has reached 169 GW, with the contribution of 16 GW from the offshore technology. An analysis of the growth of offshore and onshore wind energy in EU is available in Ref. [2]. Due to the greater social acceptance, the greater stability of the energy resource and the great potential for further development, offshore wind energy is

certainly the more promising technology in the near future, capable of reaching over 70 GW in 2030 in EU [3]. Nowadays, with a significant lag, China and US have made first steps toward offshore wind energy [4], and there are promising studies also on the potential of South-eastern Asia [5] and African coasts [6].

Most of the existing EU offshore wind farms are installed in the North Sea, where shallow water sea depth allows for the bottom fixed monopile technology. Despite its wide development, the need to move towards a deeper sea with greater abundance and less intermittence of the energy resource, through the use of floating offshore wind turbine technology (FOWT), is widely believed. The use of larger wind turbines, with power up to 12 MW and rotor diameters of about 220 m, would enable lower energy cost [3]. The technological trend of offshore wind turbines is aiming at ever larger extracted power and rotor diameter, also because they are not affected by strong spatial planning constraints.

* Corresponding author. Department of Engineering, Roma Tre University, Via Della Vasca Navale 79, 00146, Rome, Italy.

E-mail address: massimo.gennaretti@uniroma3.it (M. Gennaretti).

Nomenclature	
$\mathbf{A}_\infty, \mathbf{E}, \mathbf{F}, \mathbf{G}$	Floating Offshore Wind Turbine model RMA matrices
$\mathbf{A}, \mathbf{B}, \mathbf{C}, \mathbf{D}$	state-space FOWT model matrices
$\overline{\mathbf{A}}, \overline{\mathbf{B}}, \overline{\mathbf{C}}, \overline{\mathbf{D}}$	multiblade state-space FOWT model matrices
\mathbf{B}_{d+}	viscous damping matrix
DoF	Degree of Freedom
EU	European Union
f	wave propagation function
\mathbf{f}, \mathbf{f}_m	individual-blade and multiblade state-space forcing terms
$\mathbf{f}_{dif}, \mathbf{f}_{rad}$	hydrodynamic diffraction and radiation forces
\mathbf{f}_{d+}	hydrodynamic additional linear viscous damping loads
\mathbf{f}_{ml}	mooring lines forces
FOWT	Floating Offshore Wind Turbine
H	wave height
\mathbf{H}_{rad}	transfer function matrix of hydrodynamic radiation loads
\mathbf{H}_{ml}	transfer function matrix of mooring lines loads
J	LQR objective function
JONSWAP	JOint North Sea WAve Project
\mathbf{K}	LQR controller gain matrix
LCoE	Levelized Cost of Energy
LQR	Linear Quadratic Regulator
$\mathbf{M}_{ml}, \mathbf{C}_{ml}, \mathbf{K}_{ml}$	equivalent mass, damping and stiffness matrices of mooring lines
MWF	Mean Wave Frequency
NREL	National Renewable Energy Laboratory
P	generated power
PSD	Power Spectral Density
\mathbf{q}	platform degrees of freedom
\mathbf{Q}, \mathbf{R}	LQR weight matrix
\mathbf{r}	additional hydrodynamic states
RMA	Rational Matrix Approximation
$S, \widehat{S},$	JONSWAP and two-dimensional wave spectra
T	wave period
$\mathbf{T}, \mathbf{T}_x, \mathbf{T}_u$	multiblade transformation matrices
TLP	Tension Leg Platform
\mathbf{u}, \mathbf{u}_m	individual-blade and multiblade control vectors
\mathbf{x}, \mathbf{x}_m	individual-blade and multi-blade state variables vectors
\mathbf{y}, \mathbf{y}_m	individual-blade and multi-blade outputs vectors
β_i	i -th blade flapping degree of freedom
$\beta_0, \beta_s, \beta_c$	rotor collective, sine-cyclic and cosine-cyclic flapping degrees of freedom
θ	direction of propagation of wave components
τ	generator torque
Ψ_i	azimuth position of i -th blade
Ω	rotor speed

Anyway, this trend is confirmed also by the projects of existing onshore wind farms repowering [7]. Despite until a few years ago 10 MW was considered the technological frontier [8], nowadays, General Electric is developing a 12 MW turbine, Haliade-X. The floating platform technology still requires a great deal of research effort, stimulating an acceleration of innovative solutions capable of optimizing the efficiency of even larger floating wind turbines and facilitate the reduction of installation, operation and maintenance costs. An in-depth review concerning technological, industrial and policy issues of offshore wind energy in deep waters is provided in Ref. [9], whereas an examination of the technological effects of wind turbine repowering is presented in Ref. [7].

The Mediterranean Sea is an area of interest for the floating wind turbine farms, because of the large water depth and the energy resource stability [10]. Although the average wind power does not reach the high value of the North Sea, the milder sea-weather conditions enables the Med sea as an attractive site for testing the floating wind turbine technology. By taking into account for the above environmental factors, it will be imperative to look at innovative solutions based on the use of new materials, bioinspired hydro and aerodynamic shapes, optimized control strategies, to significantly reduce the levelized cost of energy (LCoE).

The floating wind turbine concepts currently explored are mostly inspired by the oil and gas technology, *i.e.*, spar buoy, tension-leg platform (TLP) and semi-sub platforms [11]. From the theoretical point of view, the problem is quite complex, requiring the coupled solution of aerodynamic (wind turbine) and hydrodynamic (floating platform) problems, along with the modeling of the mooring lines and of the servo-mechanic behavior of the turbine [12].

A wide literature is available in the field of comprehensive numerical modeling of FOWTs for design purposes. Significant outputs are provided by the OC5 project: Phase II focused on accurate validation of the proposed numerical solvers against 1/50 model scale experiments [13], while Phase III extended the validation to the full scale data of the Senvion 5 MW wind turbine installed in the Alpha Ventus offshore wind farm [14]. A detailed outline of the application of the open source solver FAST to the analysis of the DeepCWind triangular shaped semi-sub platform is provided in Refs. [15]. Many authors have focused their

attention on specific modeling issues of wind turbines, like unsteady aerodynamics [16], wake effects in a wind farm [17], mooring dynamics [18], interactions among adjacent wind turbines [19], or the stochastic load effects on floating support structures [20], that are of particular interest for fatigue life prediction.

Most of FOWT solvers available in literature are based on linear (inviscid) hydrodynamics models developed under small platform motion assumption [12], or blended methods where nonlinear contributions from the Froude-Krylov and hydrostatic terms are included [21]. Effects related to additional physical phenomena, like viscous drag or nonlinear wave-induced loads, are introduced through suitable nonlinear correction models. A second-order consistent model, based on the weak-scatterer approximation, has been used in Ref. [22] for the determination of nonlinear contributions to the response of a floating vessel in waves with inclusion of highly nonlinear water-on-deck and slamming loads through a blended method, and applied, for the first time, in Ref. [23] to a spar-buoy torus combination, showing a satisfactory agreement with the experimental data. Instead, a quadratic transfer function approach has been used in Ref. [24] for a TLP floating wind turbine.

The research activity and outcomes presented in this paper are part of a farsighted research project which faces with the new challenges introduced by the development of the Floating Offshore Wind Turbine (FOWT) technology. The expertise in aero/servo-elasticity of rotorcraft [25] and wind turbine modeling [26] is combined with the expertise in the nonlinear dynamics of floating platforms in waves [27], to propose an efficient and innovative prediction tool suitable for FOWTs dynamics prediction and synthesis of control laws.

The control objectives change with the operational zone of the wind turbine. For instance, in the wind speed range between the cut-in wind speed and the rated wind speed (operational region II) the typical control objective is the maximization of the generated power. Conversely, above the rated wind speed (operational region III) the control objectives are the limitation of the generated power (to avoid electrical and/or mechanical damages) and the reduction of the fluctuation of generated power and structural loads [28]. This is true for floating offshore wind turbines, as well. These operate in a harsher environment, with the additional disturbance due to waves, and are subject to low-frequency

platform/buoy motion that may give rise to instabilities [29] (for instance, a closed loop instability caused by platform dynamics and pitch controller coupling has been examined through the pole placement technique in Ref. [30]).

In the present work, an optimal control strategy for the operational region III is applied, based on the developed FOWT dynamic model. In region III most of the commercial wind turbines actually use a proportional-integral collective blade pitch controller to regulate rotor speed [28]. However, due to the movement of the platform, each FOWT blade is generally subject to aerodynamic loads which, at any instant of time, are different from those acting on the rest of the rotor blades. So an individual pitch control strategy [31] seems to be more effective. Here, a Linear Quadratic Regulator (LQR) for the minimization of power fluctuations, relying on the actuation of blade collective pitch, cyclic pitch, and generator torque is proposed. The controller synthesis is based on a linearized state-space FOWT model that couples mooring lines, platform and wind turbine mechanics.

The verification of the capability of the solver to predict FOWT dynamics, as well as the assessment of robustness and effectiveness of the proposed FOWT control strategy are carried out through an extensive numerical investigation. It concerns applications to a NREL 5-MW FOWT concept in regular and irregular short-crested sea waves. The corresponding results are shown and discussed at the end of the paper.

2. Floating offshore wind turbines dynamics

The FOWT dynamics is modeled through the multibody solver Simscape developed by Mathworks [32]. The multibody is a convenient approach due to the complex kinematics of the system and the multi-physics nature of the problem (involving aerodynamics, hydrodynamics, structural dynamics, power conversion and control actuation systems).

The multibody model is composed of the floating platform (namely, platform and mooring lines), the wind turbine tower, the nacelle, the rotor hub and the rotor blades. The wind turbine tower is assumed to be rigidly connected to the platform, and these are both assumed to be rigid bodies. The hub and the nacelle are included as concentrated masses located at the top of the tower. The blades are considered as flapping rigid bodies, with elastic effects modeled by hinges equipped with springs located at the blade roots. The spring stiffness is calculated to reproduce the first natural flapping frequency of the real blade. Three torsional hinges are included at the roots of the blades for application of the blade pitch control. The proposed structural model is suitable for synthesis and validation of a controller for generated power and aero-hydro-mechanics stability performance (a review of the state of the art of wind turbines aeroelastic modeling is available in Ref. [33]).

Air loads (aerodynamic forces on the wind turbine) and water loads (hydrodynamic forces on the floating platform) are modeled as outlined in the following.

2.1. Aerodynamic loads on wind turbine

The aerodynamic loads acting on the blades are evaluated through a blade element method [34]. It consists of a strip-theory model, for which each blade is divided into a finite number of independent segments along the span, with aerodynamic coefficients (for lift, drag and torque moment) evaluated through a lookup table approach based on the angle of attack with respect to the relative wind velocity. The integration of the sectional loads distribution yields forces and moments on the turbine [35].

To provide an accurate determination of the relative wind, the effects of wind shear, tower shadow and wake vorticity released by the lifting blades are taken into account. Specifically, the wind shear effect due to the ocean boundary layer is modeled through the widely-used logarithmic shape [36] which gives the wind speed at any height from the tower base, through knowledge of the wind speed at a reference height (for instance, the wind speed at the anemometer height). Instead, the

wind velocity defect due to the tower shadow is determined from the potential flow solution around an infinite cylinder of radius equal to that of the pylon section located at the height of the blade section passage [37]. The effects of the velocity induced by the wake vorticity are included through application of a widely-used dynamic inflow formulation [38], derived from the Pitt-Peters model [39].

Once the relative wind speed is determined by combining blade kinematics, tower kinematics, wind velocity and these correction effects, the angle of attack at each blade section is evaluated and, from the corresponding aerodynamic coefficients, the blade loads are calculated.

2.2. Platform loads

The platform supporting the wind turbine tower is assumed to be a rigid-body structure with six degrees of freedom (surge, sway, heave, roll, pitch, yaw) collected in the vector \mathbf{q} , forced by the aerodynamic and inertia loads from the wind turbine, the mooring lines connection loads, and the sea loads. The diffraction and radiation sea loads are predicted by a linear potential flow formulation, whereas viscous loads are included in approximated way.

Specifically, diffraction and radiation loads, \mathbf{f}_{dif} and \mathbf{f}_{rad} , are determined using a frequency-domain hydrodynamic solver [40]. According to Cummins [41], the linear radiation loads in the time domain are given by a convolution integral of \mathbf{q} , due to the memory effects deriving from the free-surface deformation. This implies that the transfer function between \mathbf{q} and \mathbf{f}_{rad} is of transcendental type and that, therefore, it must be suitably approximated for state-space applications (see following section).

The viscous loads are evaluated through a strip-theory approach based on the application of the Morison formulation that yields the force per unit length as a function of the platform-fluid relative motion (through a drag coefficient). However, as discussed in Ref. [42], the damping effect derived by the linear potential theory combined with the viscous drag do not provide a satisfactory prediction of the real hydrodynamic damping affecting the platform motion. Therefore, following [42], in the FOWT simulation tool an additional linear damping term is included. It is based on the following model

$$\mathbf{f}_{d+} = -\mathbf{B}_{d+}\dot{\mathbf{q}}$$

where the matrix \mathbf{B}_{d+} collects damping coefficients for surge, sway, heave and yaw motion (additional damping is negligible for roll and pitch). These coefficients are determined from the best fitting of the experimental free-decay motion of the platform [42].

The effects of the mooring lines are modeled through the open-source, multibody tool MoorDyn [43]. As highlighted in Ref. [44], multibody approaches are able to predict large amplitude mooring line dynamics, including the effects of inertial loads, hydrodynamic loads and elastic damping loads, at a limited computational cost.

The mean wave and slow-drift loads play a significant role in the accurate evaluation of surge and sway motions of the platform and of the mooring lines loads, as well. They are related to the nonlinear behavior of the wave loads, and are not considered in the present study.

3. Floating offshore wind turbines state-space modeling and control

Among the loads acting on the FOWT, blade aerodynamic forces and hydrodynamic radiation forces are characterized by complex memory effects which require specific modeling.

Unsteady aerodynamics memory effects of lifting bodies are related to the inflow velocity induced by the vorticity released by blade trailing edge and convected along the wake, whereas hydrodynamic memory effects are due to the deforming free-surface shape.

The dynamics of systems with memory effects is described by transcendental transfer functions, or convolution integrals in the time

domain. This occurs because of the presence of internal dynamics effects that are not directly described by the degrees of freedom, and hence require the introduction of additional states in a state-space representation of the system.

In our problem, a state-space formulation is needed for stability analysis and control-law design. The wake inflow is predicted through the inflow states of the modified Pitt-Peters dynamic inflow model mentioned above [38]. The state-space representation of the hydrodynamic radiation forces, as well as the reduced-order, state-space modeling of the loads exerted by the mooring lines are described in the following.

3.1. State-space model of hydrodynamic radiation forces

The state-space representation of the hydrodynamic radiation loads is derived through a three-step approach: first, the transfer function matrix relating \mathbf{q} to \mathbf{f}_{rad} is evaluated by the Cummins model [41] within a suitable frequency range of interest, then its Rational-Matrix Approximation (RMA) is determined and, finally, transformation into time domain is carried out.

Specifically, let \mathbf{H}_{rad} be the transfer function matrix of the radiation loads, such that $\tilde{\mathbf{f}}_{rad} = \mathbf{H}_{rad}(s)\tilde{\mathbf{q}}$. Its Laplace-domain RMA reads

$$\mathbf{H}_{rad}(s) \approx s^2 \mathbf{A}_\infty + s \mathbf{G}(s \mathbf{I} - \mathbf{E})^{-1} \mathbf{F} \quad (1)$$

where $(\tilde{\cdot})$ denotes Laplace-transformation and s is the Laplace variable. Since for $|s| \rightarrow \infty$ the effect of the rational component tends to vanish with respect to the quadratic component, the hydrodynamic mass matrix, \mathbf{A}_∞ , is asymptotically determined as $\mathbf{H}_{rad}(j\omega)/(-\omega^2)$, for increasing values of ω . In addition, \mathbf{E} , \mathbf{F} and \mathbf{G} are fully populated real matrices determined by a least square approach aimed at minimizing the error of the approximation of $(\mathbf{H}_{rad}(j\omega) + \omega^2 \mathbf{A}_\infty)$ in the frequency range of interest.

Finally, combining the approximated transfer matrix in Sec. 1 with the platform degrees of freedom and transforming into time domain, the radiation loads are given by the following linear, time-invariant, state-space representation

$$\begin{aligned} \dot{\mathbf{r}} &\approx \mathbf{A}_\infty \ddot{\mathbf{q}} + \mathbf{G} \mathbf{r} \\ &= \mathbf{E} \mathbf{r} + \mathbf{F} \dot{\mathbf{q}} \end{aligned} \quad (2)$$

where \mathbf{r} denotes the vector of the additional states describing the internal dynamics related to the memory effects of the water free-surface.

Even with inclusion of a relatively low number of additional variables, a state-space representation like that in Equation (2) may allow computationally efficient evaluations of the radiation forces, in very good agreement with respect to the convolution integral [45]. Moreover, it provides an explicit description of the internal hydrodynamic state dynamics, that is a crucial step for the representation of the fully-coupled, state-space system.

3.2. State-space model of mooring-line loads

In order to determine a state-space model of mooring-line loads, first the transfer function $\mathbf{H}_{ml}(s)$ relating platform motion to the corresponding forces exerted by the mooring lines, \mathbf{f}_{ml} , is identified ($\tilde{\mathbf{f}}_{ml} = \mathbf{H}_{ml} \tilde{\mathbf{q}}$). This is obtained through the mooring line dynamic responses to a suitable set of chirp-type perturbations of the platform motion, evaluated by the MoorDyn tool [43].

According to the reduced-order, state-space formulation approach of [46], the identified transfer matrix is approximated through a rational-matrix form. However, preliminary analyses have demonstrated that, in the typical frequency range of interest, there is no presence of poles, and hence the mooring-line transfer function may be suitably expressed as

$$\mathbf{H}_{ml}(s) \approx s^2 \mathbf{M}_{ml} + s \mathbf{C}_{ml} + \mathbf{K}_{ml} \quad (3)$$

thus yielding into time domain

$$\mathbf{f}_{ml}(t) \approx \mathbf{M}_{ml} \ddot{\mathbf{q}} + \mathbf{C}_{ml} \dot{\mathbf{q}} + \mathbf{K}_{ml} \mathbf{q} \quad (4)$$

Note that, because of the absence of poles, the spring matrix \mathbf{K}_{ml} may be simply determined from steady-state responses, whereas the mass and damping matrices, \mathbf{M}_{ml} and \mathbf{C}_{ml} , may be determined from the high-frequency responses to platform motion (coefficients of the real quadratic component and of the imaginary linear component, respectively).

3.3. Linearization of the fully coupled aero-hydroelastic model

For the efficient assessment of stability characteristics through the eigenanalysis approach and for controller design purposes, the FOWT dynamics is represented by a linearized, state-space form.

Here, the Linear Analysis Tool of Simscape is used to obtain the following linearized (perturbation) state-space model of the complete wind-turbine/tower/platform system about a steady-state reference configuration (corresponding to a constant-wind, no-wave condition)

$$\begin{aligned} \dot{\mathbf{x}} &= \mathbf{A}(t) \mathbf{x} + \mathbf{B}(t) \mathbf{u} + \mathbf{f} \\ \mathbf{y} &= \mathbf{C}(t) \mathbf{x} + \mathbf{D}(t) \mathbf{u} \end{aligned} \quad (5)$$

where the state variables vector, \mathbf{x} , collects the blade flapping degrees of freedom (dofs) and their time derivatives, the rotor angular velocity, the platform motion states, as well as, the aerodynamic and the hydrodynamic additional states (namely, the wake inflow states and the radiation force states, respectively). The control vector, \mathbf{u} , collects blades pitch angles and generator torque, the output, \mathbf{y} , is the generated power, whereas \mathbf{f} takes into account the external forcing terms (namely, the diffraction loads, \mathbf{f}_{df}).

Note that, the reduced-order, state-space approximation of aerodynamic and hydrodynamic operators is a prerequisite for achieving an accurate linearized representation of the system suitably taking into account the memory effects. Indeed, if the radiation forces were expressed through the original convolution integral, the application of the Linear Analysis Tool of Simscape would provide a less accurate linearized expression involving only the system dofs, without inclusion of additional states for the description of the free-surface memory effects.

Because of the periodic nature of the system due to the combination of the rotational motion of the blades with wind shear and tower aerodynamic shadow effects, the state-space matrices in Equation (5) are time-dependent. In order to obtain a more convenient time-invariant expression of the system dynamics, the Coleman transformation is applied to the blade variables [47], followed by the mean-value, constant-coefficient approximation of the resulting transformed matrices.

For a three-bladed rotor (like that examined in the numerical investigation), the Coleman transformation consists of expressing the blade flapping angle, β_i , of the i -th blade as

$$\beta_i = \beta_0 + \beta_s \sin \Psi_i + \beta_c \cos \Psi_i$$

where

$$\beta_0 = \frac{1}{3} \sum_1^3 \beta_i, \beta_s = \frac{2}{3} \sum_1^3 \beta_i \sin \Psi_i, \beta_c = \frac{2}{3} \sum_1^3 \beta_i \cos \Psi_i$$

are the so-called collective, sine-cyclic and cosine-cyclic multiblade variables evaluated at each instant of time, with Ψ_i denoting the azimuth position of the i -th blade. Thus, it is possible to define a matrix \mathbf{T} such that $\mathbf{q} = \mathbf{T} \mathbf{q}_m$, where \mathbf{q} and \mathbf{q}_m denote, respectively, the vectors collecting the (original) individual-blade and the (transformed) multiblade variables.

Then, the application of this transformation to the variables in Equation (5) yields the following multiblade state-space system

$$\begin{aligned}\dot{\mathbf{x}}_m &= \bar{\mathbf{A}} \mathbf{x}_m + \bar{\mathbf{B}} \mathbf{u}_m + \mathbf{f}_m \\ \mathbf{y} &= \bar{\mathbf{C}} \mathbf{x}_m + \bar{\mathbf{D}} \mathbf{u}_m\end{aligned}\quad (6)$$

where $\mathbf{x}_m = \mathbf{T}_x^{-1} \mathbf{x}$, $\mathbf{u}_m = \mathbf{T}_u^{-1} \mathbf{u}$ and $\mathbf{f}_m = \mathbf{T}_x^{-1} \mathbf{f}$, with \mathbf{T}_x and \mathbf{T}_u denoting the multiblade transformation matrices that transform blade flap and pitch variables appearing in \mathbf{x} and \mathbf{u} into their collective and sine-cosine cyclic components. In addition, the matrices $\bar{\mathbf{A}}$, $\bar{\mathbf{B}}$, $\bar{\mathbf{C}}$, $\bar{\mathbf{D}}$, derived by transformation of those in Equation (5) followed by constant-coefficient approximation, are described by the following expressions

$$\begin{aligned}\bar{\mathbf{A}} &= \overline{\mathbf{T}_x^{-1} (\mathbf{A} \mathbf{T}_x - \dot{\mathbf{T}}_x)}, \quad \bar{\mathbf{B}} = \overline{\mathbf{T}_x^{-1} \mathbf{B} \mathbf{T}_u}, \\ \bar{\mathbf{C}} &= \overline{\mathbf{C} \mathbf{T}_x}, \quad \bar{\mathbf{D}} = \overline{\mathbf{D} \mathbf{T}_u},\end{aligned}\quad (7)$$

The use of the multi-blade variables, constant-coefficients system of Equation (6) is a viable approach for the design of a generated power LQR controller without dealing with periodic equations [48]. Since the objective of this work is the reduction of generated power fluctuations, the output, \mathbf{y} , of the linearized system is assumed to be the perturbation, P' , of the generated power due to the external wave disturbances. Denoting with τ_0 and Ω_0 , respectively, the reference, steady-state generator torque and rotor angular velocity, and with τ' and Ω' the corresponding perturbations, P' is given by

$$P' = \tau' \Omega_0 + \tau_0 \Omega' + \tau' \Omega' \quad (8)$$

with the last nonlinear term assumed to be negligible and the remaining terms used to define the matrices $\bar{\mathbf{D}}$ and $\bar{\mathbf{C}}$ of Equation (7).

3.4. Control procedure

The purpose of the FOWT control is the alleviation of generated power perturbations due to sea-waves/platform interaction. This is achieved by blade pitch actuation and generator torque variation, as given by a proportional control law, $\mathbf{u}_m = \mathbf{K} \mathbf{x}_m$. The gain matrix \mathbf{K} is identified through a LQR approach that consists of minimizing the following objective function

$$J = \int_0^\infty (\mathbf{y}^T \mathbf{Q} \mathbf{y} + \mathbf{u}_m^T \mathbf{R} \mathbf{u}_m) dt \quad (9)$$

under the constraint of the linearized FOWT model in Equation (6), with forcing term, \mathbf{f}_m , neglected. In Equation (9), \mathbf{y} is the generated power perturbation, whereas \mathbf{Q} and \mathbf{R} are output and control weight matrices identified as those providing the best compromise between effectiveness and control effort. A similar control strategy, but limited only to blade pitch as a control input, is proposed in Refs. [49].

The controller is designed to be able to reject small perturbations due to any external action, without requiring knowledge about it (the influence of the external forcing term on the control actuation takes place through the closed-loop feedback). Recently, incident wave measurement has been proposed in a feedforward control scheme for enhancing disturbance rejection capability [50].

3.5. State observer

In principle, when a LQR is applied, the feedback to be provided for the definition of the actuation variables consists of the entire set of system state variables.

In practice, rigid-body degrees of freedom of the FOWT platform and rotor angular velocity may be easily measured (using, for instance, an inertial platform and an encoder), whereas blade flapping deformation may be measured by installation of strain gauges (and suitably correlated to an equivalent blade rigid flapping displacement).

However, the proposed FOWT dynamics formulation includes wake-inflow and radiation-force additional states that are not measurable. Therefore, the application of the LQR controller requires the introduction of an observer for the estimation of the non-measured feedback

states. To this purpose, the Luenberger state observer is included in the FOWT control chain [51].

In the controller examined in Ref. [49] neither blade dofs nor aero-hydrodynamic additional states are included in the state space model the LQR is based on, and hence it considers a fully-measurable feedback state vector.

4. Numerical results

Several floating platform and wind turbine concepts are available for modeling a FOWT.

Here, the NREL 5-MW model [52] is selected to represent the wind turbine. The inertia properties have been evaluated by integrating the mass distribution data provided in Ref. [52]; the stiffness of the blade hinge springs is evaluated so to reproduce the first flapping frequency of the prototype [52].

For the simplicity of design and modeling, a spar buoy platform is considered [42]. It is a widely-applied solution as a floating foundation for offshore wind turbines, and hence this choice is motivated also by the large amount of experimental/numerical data available. The platform is moored by a system of three catenary lines attached to the platform via a delta connection. The specific characteristics of the mooring system are given in Ref. [42].

In the following, the developed FOWT state-space model is first used for the system stability analysis of the reference condition corresponding to a uniform wind speed equal to 12.5 m/s (over rated condition) and collective pitch equal to -4.5° . A logarithmic wind profile with a roughness length of 0.001 m, and a reference height equal to the hub height (90 m) is considered.

Then, the aero/hydromechanic model is applied to examine the FOWT response and wind-extracted power in the presence of wave-induced loads. Finally, the capability of the proposed optimal control strategy to alleviate generated power fluctuations in sea waves is assessed.

4.1. Aero-hydromechanic floating offshore wind turbines stability

Once the perturbation FOWT dynamics about the reference steady operating condition is described through the linear system in Equation (6), its stability characteristics are examined by eigenanalysis of the state matrix $\bar{\mathbf{A}}$.

First, the eigenvalues computed with and without inclusion of the additional linear viscous damping terms are shown in Fig. 1 and demonstrate that the latter play a fundamental role in the FOWT stability, by avoiding unstable poles.

As shown in Fig. 2, the FOWT stability roots are affected also by the additional hydrodynamic states which, indeed, reduce the system damping. Table 1 presents the list of the lower-frequency FOWT modes (with the indication of the dominant components of the eigenvectors). It is interesting to notice that most of them are coupled modes involving

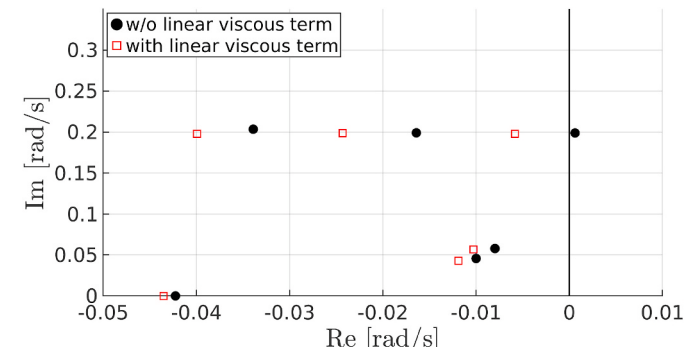


Fig. 1. FOWT poles with and w/o linear viscous damping.

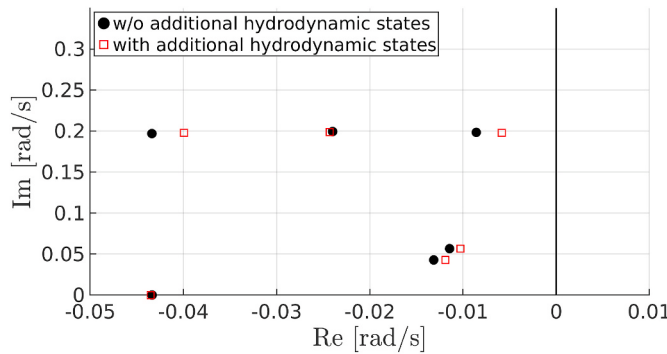


Fig. 2. FOWT poles with and w/o additional hydrodynamic states (linear viscous terms included).

Table 1
Lower-frequency FOWT modes.

Mode	Period [s]	Damping ratio [-]
rotor speed	144.43	1.0000
surge, rotor speed	141.25	0.2671
Sway	109.19	0.1787
sway, roll	31.73	0.0295
surge, heave, pitch, rotor speed	31.36	0.1213
surge, pitch, rotor speed	31.13	0.1978
wake inflow, rotor speed	14.00	1.0000
yaw, blade cyclic flap	8.35	0.4185

rotor and platform dynamics, as well as aerodynamic inflow state.

4.2. Response to regular sea waves

The nonlinear FOWT aero/hydromechanic model is used to examine the response in waves. Indeed, the spar buoy motion affects the relative velocity between air and rotor blades, thus yielding time-variant aerodynamic loads and generated power.

An incident regular wave aligned to the surge axis, with $H = 3.25$ m and $T = 7.5$ s is considered. Neither sway diffraction force nor roll and yaw diffraction moments are produced by this kind of wave configuration.

Figs. 3 and 4 depict the dynamic response of the FOWT model in terms of the spar buoy degrees of freedom (surge, sway and heave displacements are evaluated at the axis point that is 120 m distant from the bottom of the buoy). These results demonstrate that the wave loads significantly affect surge displacement and pitch and yaw rotations. The unexpected effect on the yaw rotation is due to the rotor hub yaw moment given by the combination of the out-of-phase rotor blade flap response and spar buoy pitch motion.

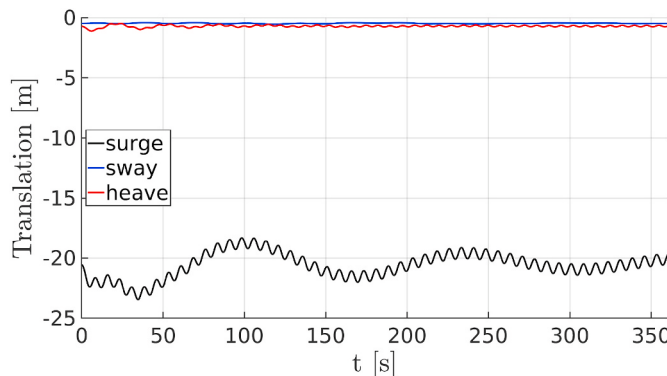


Fig. 3. Platform translation response to regular sea.

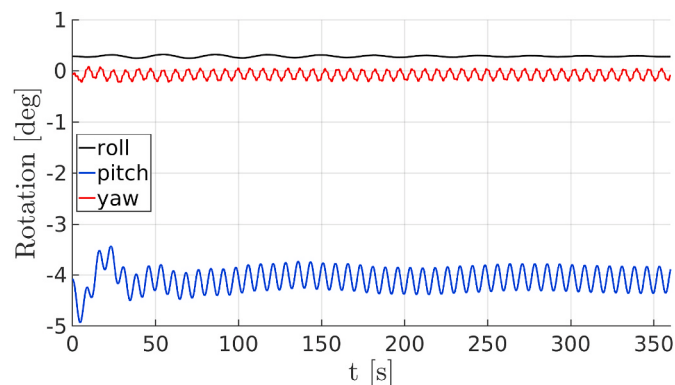


Fig. 4. Platform rotation response to regular sea.

4.3. Controlled response to regular sea waves

As already mentioned, the objective of the proposed controller is to reduce as much as possible the power fluctuations generated by the incident sea waves, through actuation of rotor blade pitch and generator torque. In order to validate the effectiveness of the developed controller, it is applied to the FOWT dynamics as predicted by the complete, nonlinear simulation model.

Fig. 5 shows that the regulator is fully capable of controlling the generated power, making the power fluctuations negligible with respect to the extracted mean value (the results are presented for the controller activated after 5 s of wave impingement). At the same time, Fig. 6 shows that also a non-negligible reduction of the wind turbine thrust is achieved, as an involuntary by-product of the control action aimed at power fluctuation alleviation. This positive effect is a consequence of the reduction of the fluctuations of the controlled aerodynamic torque.

Note that, the required control effort (power) is almost negligible, as it can be assessed from the limited amplitudes of the actuated blade pitch and rotor torque shown in Figs. 7 and 8. Note also that the FOWT dynamic response (rotor and spar buoy dofs) is only slightly affected by the control action (these results are not shown here for the sake of conciseness).

Moreover, it is worth highlighting that a second interesting by-product of the applied controller is a slightly less damped rotor-surge coupled motion, represented in Fig. 9 through the most critical pole, that does not affect appreciably the generated power.

4.4. Controlled response to irregular short-crested sea waves

In order to assess the capability of the developed controller to reject fluctuation of the generated power due to more general sea conditions, it is applied to the FOWT perturbed by a multi-harmonic, multi-directional, short-crested irregular sea waves. Specifically, a two-dimensional

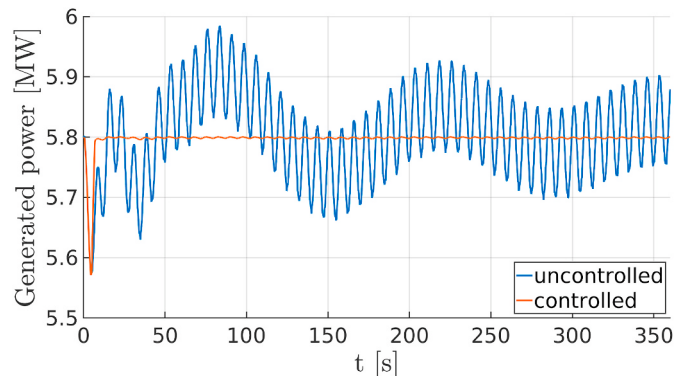


Fig. 5. Uncontrolled and controlled generated power.

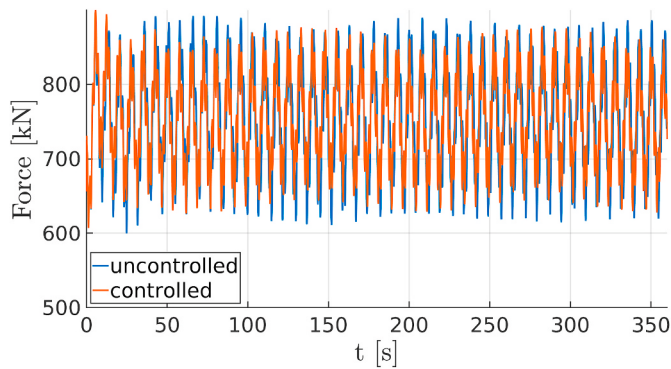


Fig. 6. Hub thrust with and without control actuation.

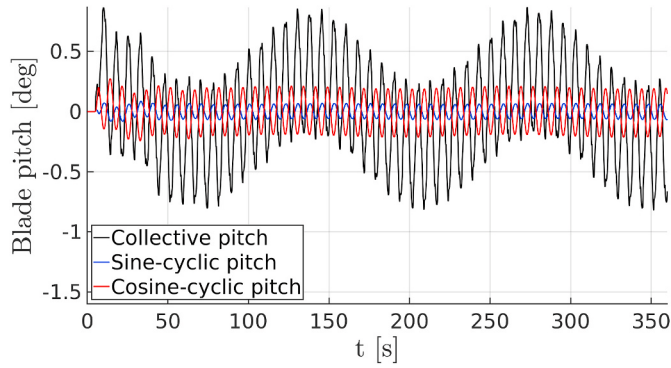


Fig. 7. Actuated blade pitch.

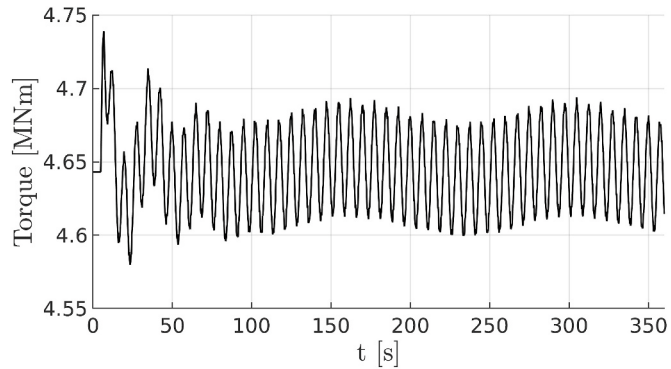


Fig. 8. Actuated rotor torque.

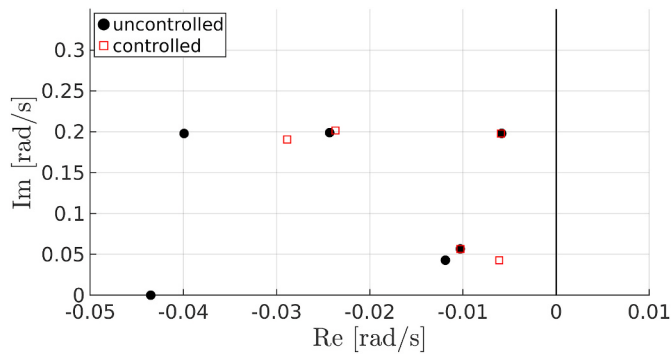


Fig. 9. Uncontrolled and controlled critical FOWT poles.

wave spectrum, $\hat{S}(\omega, \theta) = S(\omega)f(\theta)$, is considered, where $S(\omega)$ denotes the JONSWAP spectrum [53], here assumed to have characteristic height $H = 3.25$ m and characteristic period $T = 7.5$ s. In addition, for θ denoting the angle of the direction of propagation of the wave components, $f(\theta)$ represents the wave propagation function, typically assumed to be $f(\theta) = (2/\pi)\cos^2\theta, (-\pi/2) < \theta < (\pi/2)$ [54].

The Power Spectral Densities (PSDs) of the corresponding hydrodynamic diffraction loads acting on the FOWT are depicted in Figs. 10 and 11. These show a bell shape centered at the mean wave frequency (MWF) that directly derives from the JONSWAP sea state spectrum. Note that the PSD results of the parameters examined are obtained through 30-min time-marching simulations and that, for simplicity, non-linear hydrodynamic viscous terms are neglected.

Then, the effectiveness of the controller for such a perturbation load condition is proven. As for the results presented in the previous section, the controller designed through the FOWT reduced-order model is validated by inclusion in the FOWT dynamics predicted by the complete, nonlinear simulation model (this is a widely-applied validation procedure for complex systems controllers, as illustrated in Refs. [55] for helicopter dynamics applications.)

Fig. 12 presents the PSD of the generated power for both uncontrolled and controlled FOWT (solid and dashed black lines, respectively). The effect of the diffraction loads generated by the JONSWAP sea state spectrum is clearly visible around the MWF. However, additional PSD peaks appear at the multiples of the blade passing frequency (BPF), due to the combination of the unsteady loads from each blade at the hub (the dominating BPF load components are the result of the well-known rotor hub filtering effect [56]). Indeed, a significant reduction of generated power fluctuations is obtained throughout the entire frequency range examined, with inclusion of the higher BPF peaks. The comparison of the generated power with its aerodynamic component shows that the contribution by the inertial loads is remarkable (growing with frequency, as expected), and that it is strongly affected by the control action.

The capability of the proposed controller to provide good performance in a wide frequency range is demonstrated by the open-loop transfer functions between generated power and control variables depicted in Figs. 13 and 14. They show the complementary ranges of effectiveness of rotor torque and blade pitch actuation (only the collective pitch component is considered for the sake of conciseness). Indeed, for a fixed generator torque, in the low-frequency range, increasing/decreasing the blade pitch yields an increase/decrease in rotor aerodynamic torque and hence in rotor angular velocity and generated power, as well. On the other hand, since rotor inertia acts like a low-pass filter, high-frequency pitch control and corresponding aerodynamic torque scarcely affect rotor angular speed and hence generated power. Rather, for fixed blade pitch, in the low-frequency range, increasing/decreasing generated torque produces a decrease/increase of rotor angular velocity and hence scarcely affects generated power. Conversely, high-frequency generated torque increase directly yields

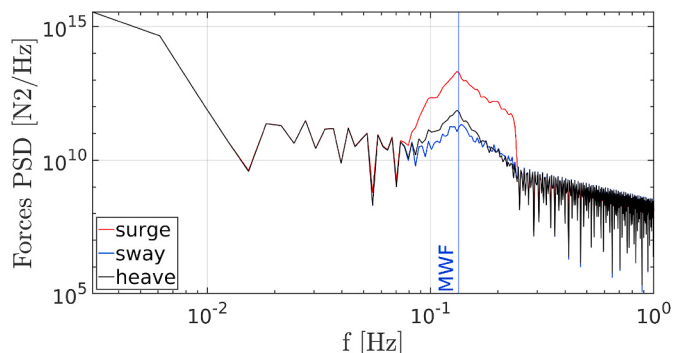


Fig. 10. Diffraction forces on the spar buoy in irregular short-crested sea wave.

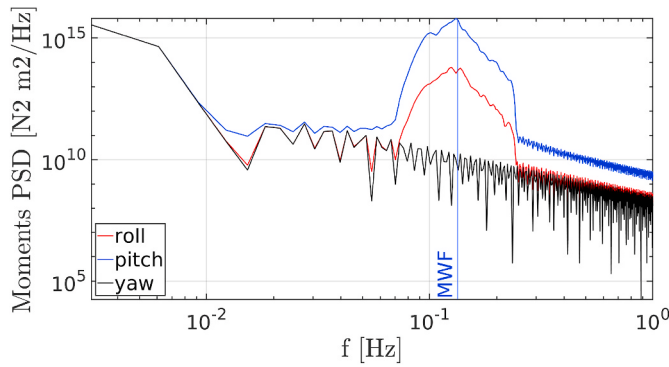


Fig. 11. Diffraction moments on the spar buoy in irregular short-crested sea wave.

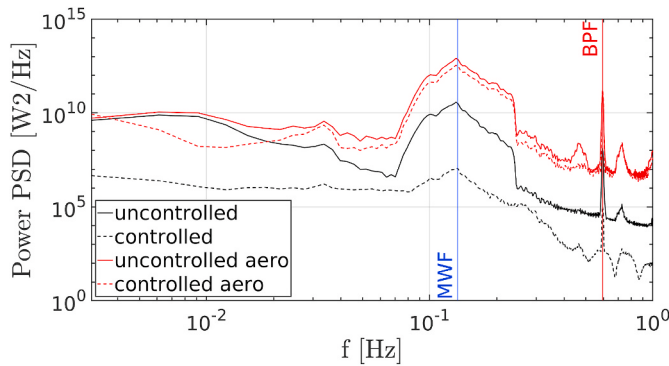


Fig. 12. Uncontrolled and controlled generated power and aerodynamic power.

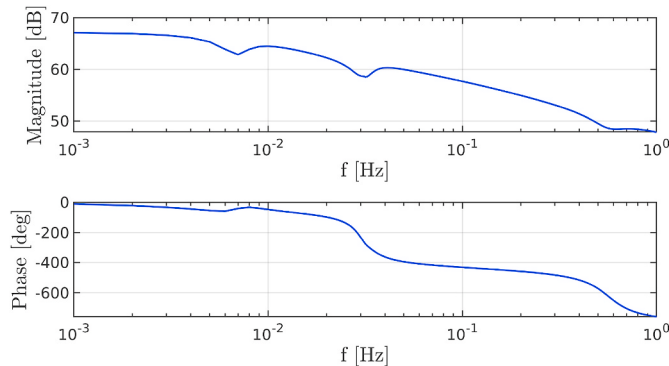


Fig. 13. Transfer functions relating generated power to collective pitch.

generated power increase, in that the rotor angular speed remains almost unaltered because of rotor inertia.

As compared to the LQR proposed in Ref. [49], the combined use of rotor blade pitch and generator torque as control inputs yields a significantly increased capability of rejection of wave-generated disturbances. A multiple-input-multiple-output controller is proposed in Ref. [57] for stabilization in region III.

As a consequence of the reduction of generated (and aerodynamic) power fluctuations, hub thrust fluctuations are alleviated (see Fig. 15) and, akin to the regular wave control, the corresponding required control effort (power) is almost negligible.

Finally, Fig. 16 shows the controlled generated power obtained both assuming all feedback states to be measurable and introducing an observer for the additional aerodynamic and hydrodynamic states. These results are practically identical, thus demonstrating the

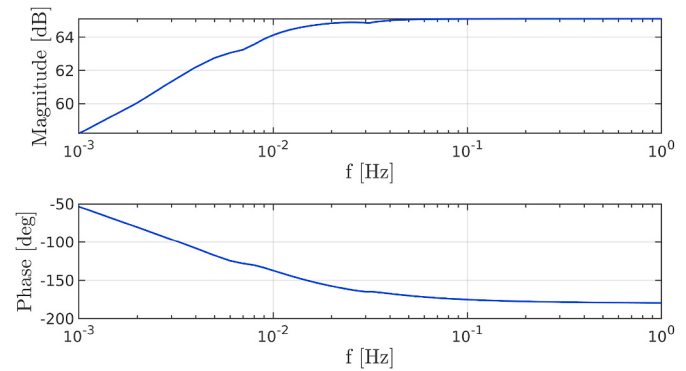


Fig. 14. Transfer functions relating generated power to generator torque. Note that, for the JONSWAP sea spectrum, generated power stabilization may efficiently be obtained through generator torque control, being the blade pitch control almost ineffective at that frequency range (compare Fig. 12 with Figs. 13 and 14). Nevertheless, applications of Proportional-Integral (PI) control strategies based on collective pitch actuation (originally introduced for onshore wind turbines) are present in the available literature [28,42]. These are not suitable for alleviation of generated power fluctuation due to irregular sea waves, while can be efficiently used for alleviation of wind perturbation effects.

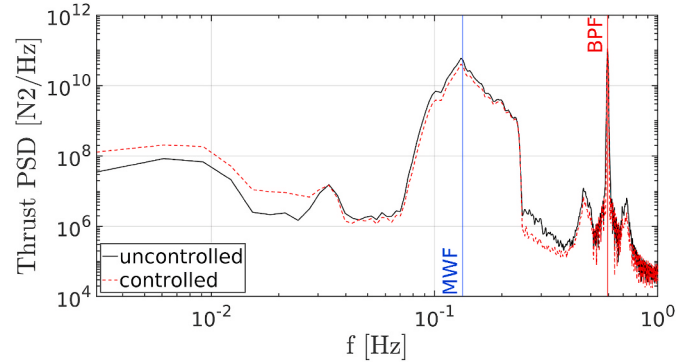


Fig. 15. Hub thrust with and without control actuation.

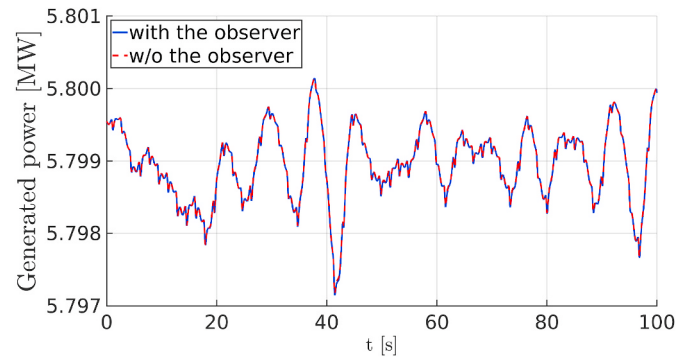


Fig. 16. Controlled generated power with and without observer.

effectiveness of the applied observation strategy.

5. Conclusions

A fully-coupled aero/hydro/servo-mechanic multibody model for FOWT stability and response analysis, as well as, for control-law synthesis has been developed. The wind turbine model predicts generated power taking into account the effects of blade elastic flapping, wind shear, tower shadow and wake inflow. The hydrodynamic loads acting

on the platform are evaluated by a first-order potential-flow solver, with inclusion of linear and nonlinear viscous corrections. Mooring lines effects on platform dynamics are also taken into account. The linearized version of the FOWT aero/hydro/servo-mechanic model has been determined and applied for stability analysis and control design purposes. It includes a state-space model of the hydrodynamics radiation forces, with memory effects related to free surface deformation taken into account through introduction of a suitable set of additional hydrodynamic states. A LQR approach has been applied for control-law synthesis, coupled with a Luenberger observer for the estimation of non-measurable states (wake inflow and hydrodynamic additional states). Numerical investigations concerning a widely-used wind turbine model with spar buoy foundation have demonstrated the capability of the proposed model to perform stability analysis in the presence of uniform wind, as well as, to predict response to regular and irregular short-crested sea waves. In addition, the application of the proposed controller to the complete, nonlinear FOWT model impinged by regular and irregular short-crested sea waves, has demonstrated its effectiveness in alleviating the corresponding (annoying) generated power fluctuations, along with vibratory loads (as a by-product). The combined use of blade pitch and generator torque as control variables makes the proposed controller able to provide good performance in a wide frequency range (because of the proven complementarity of the effectiveness frequency ranges). The capability of the applied observer to estimate non-measurable aerodynamic and hydrodynamic states has been demonstrated, as well. Concerning the FOWT stability, the beneficial effects of actuated control and hydrodynamic viscous terms has been assessed. Thanks to the modular scheme applied for the definition of the aero/hydro/servo-mechanic FOWT model based on reduced-order structural dynamics, aerodynamics and hydrodynamics models, the inclusion of higher-fidelity modeling components is a feasible task for future developments of the present work.

Acknowledgments

The research leading to the results of this paper is supported by the Italian Ministry of Economic Development under the Grant Agreement “RdS PTR 2019–2021 - Energia elettrica dal mare”. This work (for C. Lugni) was supported also by the Ministry of Science and Technology of P. R. China. (G20190008061) and the Ministry of Industry and Information Technology of P. R. China (Numerical Tank Project). C. Lugni was also supported by the Research Council of Norway through the Centers of Excellence funding scheme AMOS, project number 223254.

References

- [1] Directorate-general for energy. Clean energy for all europeans. Tech. Rep. MJ-03-19-092-EN-N. European Union; 2019.
- [2] Bilgili M, Yasar A, Simsek E. Offshore wind power development in europe and its comparison with onshore counterpart. *Renew Sustain Energy Rev* 2011;15(2):905–15.
- [3] Offshore wind temporary working group. Offshore wind implementation plan. Tech. Rep.. EU-SET Plan; 2018.
- [4] DeCastro M, Salvador S, Gómez-Gesteira M, Costoya X, Carvalho D, Sanz-Larruga F, et al. Europe, China and the United States: three different approaches to the development of offshore wind energy. *Renew Sustain Energy Rev* 2019;109:55–70.
- [5] VV.Aa.. Offshore wind outlook 2019. Tech. Rep.. International Energy Agency; 2019.
- [6] Elsner P. Continental-scale assessment of the african offshore wind energy potential: spatial analysis of an under-appreciated renewable energy resource. *Renew Sustain Energy Rev* 2019;104:394–407.
- [7] Lacaí-Arántegui R, Uihlein A, Yusta JM. Technology effects in repowering wind turbines. *Wind Energy* 2020;23(3):660–75.
- [8] Ederer N. The right size matters: investigating the offshore wind turbine market equilibrium. *Energy* 2014;68:910–21.
- [9] Bento N, Fontes M. Emergence of floating offshore wind energy: technology and industry. *Renew Sustain Energy Rev* 2019;99:66–82.
- [10] Zountouridou E, Kiokes G, Chakalis S, Georgilakis P, Hatzigyrgiou N. Offshore floating wind parks in the deep waters of mediterranean sea. *Renew Sustain Energy Rev* 2015;51:433–48.
- [11] Liu Y, Li S, Yi Q, Chen D. Developments in semi-submersible floating foundations supporting wind turbines: a comprehensive review. *Renew Sustain Energy Rev* 2016;60:433–49.
- [12] Jonkman JM. Dynamics of offshore floating wind turbines—model development and verification. *Wind Energy: An International Journal for Progress and Applications in Wind Power Conversion Technology* 2009;12(5):459–92.
- [13] Robertson AN, Wendt F, Jonkman JM, Popko W, Dagher H, Gueydon S, et al. OC5 project phase II: validation of global loads of the deepCwind floating semisubmersible wind turbine. *Energy Procedia* 2017;137:38–57.
- [14] Popko W, et al. Validation of numerical models of the offshore wind turbine from the alpha ventus wind farm against full-scale measurements within OC5 phase III. In: International conference on offshore mechanics and arctic engineering, vol. 10. Ocean Renewable Energy; 2019. OMAE2019-95429, V010T09A065.
- [15] Coulling AJ, Goupee AJ, Robertson AN, Jonkman JM, Dagher HJ. Validation of a FAST semi-submersible floating wind turbine numerical model with deepCwind test data. *J Renew Sustain Energy* 2013;5(2):023116.
- [16] Tran TT, Kim DH. The platform pitching motion of floating offshore wind turbine: a preliminary unsteady aerodynamic analysis. *J Wind Eng Ind Aerod* 2015;142:65–81.
- [17] Jonkman J, Doubrawa P, Hamilton N, Annoni J, Fleming P. Validation of FAST farm against large-eddy simulations. In: *Journal of physics: conference series*, vol. 1037. IOP Publishing; 2018, 062005.
- [18] Wendt F, Robertson A, Jonkman J, Andersen MT. Verification and validation of the new dynamic mooring modules available in FAST v8. Tech. Rep.. Golden, CO (United States): National Renewable Energy Lab.(NREL); 2016.
- [19] Yu Z, Zheng X, Ma Q. Study on actuator line modeling of two NREL 5-MW wind turbine wakes. *Appl Sci* 2018;8(3):434.
- [20] Okpalororo S, Sriramula S. Stochastic load effect characterization of floating wind turbine support structures. In: *Journal of physics: conference series*, vol. 1356. IOP Publishing; 2019, 012013.
- [21] Philippe M, Babarit A, Ferrant P. Aero-hydro-elastic simulation of a semi-submersible floating wind turbine. *J Offshore Mech Arctic Eng* 2010;136.
- [22] Greco M, Lugni C. 3-d seakeeping analysis with water on deck and slamming. part 1: numerical solver. *J Fluid Struct* 2012;33:127–47.
- [23] Wan L, Greco M, Lugni C, Gao Z, Moan T. A combined wind and wave energy-converter concept in survival mode: numerical and experimental study in regular waves with a focus on water entry and exit. *Appl Ocean Res* 2017;63:200–16. <https://doi.org/10.1016/j.apor.2017.01.013>.
- [24] Roald L, Jonkman J, Robertson A, Chokani N. The effect of second-order hydrodynamics on floating offshore wind turbines. *Energy Procedia* 2013;35:253–64.
- [25] Molica Colella M, Bernardini G, Gennaretti M. Tiltrotor wing-root vibratory loads reduction through higher harmonic control actuation. *J Aircraft* 2012;49:1813–20.
- [26] Calabretta A, Molica Colella M, Greco L, Gennaretti M. Assessment of a comprehensive aeroelastic tool for horizontal-axis wind turbine rotor analysis. *Wind Energy* 2016;19:2301–19.
- [27] Lugni C, Greco M, Faltinsen OM. Influence of yaw-roll coupling on the behavior of a FPSO: an experimental and numerical investigation. *Appl Ocean Res* 2015;51:25–37. <https://doi.org/10.1016/j.apor.2015.02.005>.
- [28] Njiri JG, Soeffker D. State-of-the-art in wind turbine control: trends and challenges. *Renew Sustain Energy Rev* 2016;60:377–93.
- [29] Salic T, Charpentier JF, Benbouzid M, Le Boulluec M. Control strategies for floating offshore wind turbine: challenges and trends. *Electronics* 2019;8(10):1185.
- [30] Larsen TJ, Hanson TD. A method to avoid negative damped low frequent tower vibrations for a floating, pitch controlled wind turbine. In: *Journal of physics: conference series*, vol. 75. IOP Publishing; 2007. p. 12073.
- [31] Bossanyi EA. Individual blade pitch control for load reduction. *Wind Energy: An International Journal for Progress and Applications in Wind Power Conversion Technology* 2003;6(2):119–28.
- [32] The Mathworks I. MATLAB version 9.7.0.1216025 (R2019b) Update 1. 2019. Natick, Massachusetts.
- [33] Wang L, Liu X, Koliros A. State of the art in the aeroelasticity of wind turbine blades: aeroelastic modelling. *Renew Sustain Energy Rev* 2016;64:195–210.
- [34] Bramwell A RS, Balmford D, Done G. Bramwell's helicopter dynamics. Oxford, UK: Butterworth-Heinemann; 2001.
- [35] Gupta S, Leishman J. Comparison of momentum and vortex methods for the aerodynamic analysis of wind turbines. In: 43rd AIAA aerospace sciences meeting and exhibit; 2005. p. 594.
- [36] Veritas DN. Dnv-os-j101-design of offshore wind turbine structures. Det Norske Veritas; 2004.
- [37] Sørensen P, Hansen AD, Rosas PAC. Wind models for simulation of power fluctuations from wind farms. *J Wind Eng Ind Aerod* 2002;90(12–15):1381–402.
- [38] Leishman GJ. Principles of helicopter aerodynamics with CD extra. Cambridge university press; 2006.
- [39] Pitt DM, Peters DA. Theoretical prediction of dynamic inflow derivatives. *Vertica* 1981;5(1).
- [40] Landrini M, Lugni C. Dynamics of the floating structures. part i: linear analysis in the frequency domain. Tech. Rep.. INSEAN; 1996.
- [41] Cummins W. The impulse response function and ship motions. Tech. Rep.. David Taylor Model Basin Washington DC; 1962.
- [42] Jonkman J. Definition of the floating system for phase iv of oc3. Tech. Rep.. Golden, CO (United States): National Renewable Energy Lab.(NREL); 2010.
- [43] Hall M. Moordynâ“ users guide. Orono, ME, USA: Department of Mechanical Engineering, University of Maine; 2015.

- [44] Borg M, Collu M, Kolios A. Offshore floating vertical axis wind turbines, dynamics modelling state of the art. part ii: mooring line and structural dynamics. *Renew Sustain Energy Rev* 2014;39:1226–34.
- [45] Borg M, Collu M. Offshore floating vertical axis wind turbines, dynamics modelling state of the art. part iii: hydrodynamics and coupled modelling approaches. *Renew Sustain Energy Rev* 2015;46:296–310.
- [46] Gennaretti M, Gori R, Serafini J, Cardito F, Bernardini G. Identification of rotor wake inflow finite-state models for flight dynamics simulations. *CEAS Aeronautical Journal* 2017;8(1):209–30.
- [47] Bir G. Multi-blade coordinate transformation and its application to wind turbine analysis. In: 46th AIAA aerospace sciences meeting and exhibit; 2008. p. 1300.
- [48] Stol K, Balas M. Full-state feedback control of a variable-speed wind turbine: a comparison of periodic and constant gains. *J Sol Energy Eng* 2001;123(4):319–26.
- [49] Lemmer F, Schlipf D, Cheng PW. Control design methods for floating wind turbines for optimal disturbance rejection. In: *Journal of physics: conference series*, vol. 753. IOP Publishing; 2016. p. 92006.
- [50] Al, M., Fontanella, A., van der Hoek, D., Liu, Y., Belloli, M., van Wingerden, J.W.. Feedforward control for wave disturbance rejection on floating offshore wind turbines. arXiv preprint arXiv:200402931 2020;.
- [51] Friedland B. *Control system design: an introduction to state-space methods*. New York, NY, USA: Dover Publications, Inc.; 2005.
- [52] Jonkman J, Butterfield S, Musial W, Scott G. Definition of a 5-MW reference wind turbine for offshore system development. Tech. Rep.. Golden, CO (United States): National Renewable Energy Lab.(NREL); 2009.
- [53] Hasselmann K, Barnett TP, Bouws E, Carlson H, Cartwright DE, Enke K, et al. Measurements of wind-wave growth and swell decay during the joint north sea wave project (JONSWAP). *Ergnzungsheft zur Deutschen Hydrographischen Zeitschrift Reihe* 1973;A8(12).
- [54] Faltingsen O. *Sea loads on ships and offshore structures*, vol. 1. Cambridge university press; 1993.
- [55] Hu J, Gu H. Survey on flight control technology for large-scale helicopter. *International Journal of Aerospace Engineering* 2017;14. Article ID 5309403.
- [56] Johnson W. *Rotorcraft aeromechanics*, vol. 36. Cambridge University Press; 2013.
- [57] Fischer B. Reducing rotor speed variations of floating wind turbines by compensation of non-minimum phase zeros. *IET Renew Power Gener* 2013;7(4): 413–9.